Hindawi
Journal of Nanomaterials
Volume 2019, Article ID 5287632, 10 pages
https://doi.org/10.1155/2019/5287632

Research Article

Synthesis, Characterization, and In Situ Antifungal and Cytotoxicity Evaluation of Ascorbic Acid-Capped Copper Nanoparticles

Ernesto Beltrán-Partida,[1] Benjamín Valdez-Salas,[1] Ernesto Valdez-Salas,[1] Guillermo Pérez-Cortéz,[2] and Nicola Nedev[1]

[1]*Laboratorio de Biología Molecular y Cáncer, Instituto de Ingeniería, Universidad Autónoma de Baja California, Mexico*
[2]*Facultad de Odontología Mexicali, Universidad Autónoma de Baja California, Mexico*

Correspondence should be addressed to Benjamín Valdez-Salas; benval@uabc.edu.mx

Received 2 August 2018; Revised 5 October 2018; Accepted 17 October 2018; Published 17 February 2019

Academic Editor: Simo-Pekka Hannula

The design route, synthesis, and characterization of spherical copper nanoparticles with antifungal potential are reported in the present work. Copper nanoparticles were synthesized by a novel, inexpensive, and eco-friendly chemical reduction method using ascorbic acid as a reductant and stabilizer under reflux conditions. The characterization results showed the formation of homogeneous, dispersed, and stable spherical ascorbic acid-capped copper nanoparticles (CuNPs) with a diameter of 250 nm. The CuNPs exhibited sustained antifungal activity against *Candida albicans* (*C. albicans*) after 24 h and even 48 h of incubation. Using enhanced dark-field microscopy, we presented the in situ interaction between CuNPs and *C. albicans*. Here, part of the interaction of CuNPs among the *C. albicans*, studied without the use of any chemical and/or physical fixing method, is discussed. The results indicate that part of the antifungal mechanism involves a promoted adhesion of CuNPs onto the cell wall and a massive accumulation of CuNPs into the fungal cells, concluding in cellular leakage. The cytotoxicity (viability) evaluations indicated that our CuNPs were more biocompatible after comparison to the Cu precursor and triclosan (a commercial antifungal drug). The synthesized CuNPs will open up a new road for their possible use as a potent antimicrobial agent for clinical and industrial applications.

1. Introduction

Localized, systemic, and chronic infection diseases are mainly caused by critical propagation of antibiotic/antifungal resistant strains [1], which can result in the formation of a viable biofilm and promote by this way higher resistance to conventional chemotherapeutic treatments [2]. Moreover, clinical and microbiological studies have suggested important deficiencies of the first-line antimicrobial agents selected as therapeutic tools [3, 4]. Results from dangerous clinical infections are (but not limited to) surgical wound illnesses, inflammations, immunological diseases, and even dental pathologies that in certain cases conclude mortal sepsis [5]. On the basis of dental infections, *C. albicans* has been considered the main opportunistic fungal cell present in the mouth [6]. However, *C. albicans* not only is limited to the oral cavity but also is frequently able to colonize the skin, gastrointestinal and urogenital tracts, and HIV-infected and immunosuppressed patients and in the worst case causes invasive candidiasis (candidemia, mortality rate over 60%) [6–8]. This important information regards the need for more effective antimicrobial agents with especial antifungal activity.

It is widely known that copper (Cu) presents interesting antimicrobial activity against a wide number of microbial strains. Moreover, when bulk Cu is transformed to CuNPs, the physicochemical and biological properties of Cu can be improved (e.g., the catalytic, optical, electrical, and more importantly the antimicrobial capability) [9]. Several strategies have been explored in order to synthesize CuNPs, for example, laser ablation, thermal modifications, vacuum vapor

deposition, and chemical reduction [10–12]. Interestingly, chemical reduction offers a versatile and easy way to synthesize reproducible, stable, and controllable CuNPs, by the reduction and stabilization of Cu^{+2} ions to Cu^0 by capping with organic compounds (if the synthesis is carried out under reflux conditions) [13, 14]. However, the most proposed reduction protocols use costly reducer and stabilizer agents, toxic and pollutants reagents (which are difficult to eliminate from the chemical reactions and expensive to discard), and complicated synthetic protocols that require extreme temperatures or even the application of inert atmospheres [9, 15–17]. Taking together this information, the need of novel synthetic routes for the development of CuNPs using cost-effective, eco-friendly, and facile approaches with promising antifungal capability must be highlighted.

There have been extensive reports analyzing the antimicrobial action mechanism of different metallic nanoparticles. In a recent study, Yan et al. suggested that the antibacterial activity of silver nanoparticles (AgNPs) against *Pseudomonas aeruginosa* is in part mediated by intracellular generation of reactive oxygen species (ROS) and dysfunction of the cell membrane integrity [18]. Moreover, a transmission electron microscopy (TEM) analysis proposed that AgNPs are capable to attach to the surface of the cell membrane of *Escherichia coli* (*E. coli*) and consequently penetrate inside the cell resulting into lysis [19]. On the other hand, it was reported that CuNPs presented antibacterial activity to eradicate *Staphylococcus aureus* (*S. aureus*) via destabilization and permeabilization of the cell membrane [20]. However, those studies evaluated the behavior and diffusion of nanoparticles (NPs) into bacterial cells using fixing and destructive characterization techniques (microscopically and/or molecular), which did not offer accurate in situ results. As far as the literature compendium is growing, there are still a lacking number of studies evaluating the antifungal activity of CuNPs, with special attention in the analysis of the action mechanism without applying fixing or special sample preparations.

The aim of the present work was to synthesize reproducible and homogenous CuNPs (≈250 nm) with potent antifungal capability (instead of the mainly studied antibacterial action) and controlled cytotoxicity (using a human model of fibroblasts for viability essay) by developing a new, facile, eco-friendly, and cost-effective chemical reduction approach. Moreover, this study addresses a part of the antifungal mechanism of the CuNPs against *C. albicans* using a Cytoviva® system, as a sophisticated characterization technique that allows the in situ evaluation of cell-NP interaction without applying any chemical and/or physical expensive fixing procedure (preserving the cellular integrity and free of artifacts).

2. Materials and Methods

2.1. Synthesis of CuNPs. The synthesis of CuNPs was performed by a novel, eco-friendly, cost-effective, simple, and reproducible chemical reduction method without the need of inert atmospheric conditions. As a Cu precursor, an aqueous solution of copper carbonate ($CuCO_3$ 0.134 M, Sigma-Aldrich, USA) was heated at 80°C under atmospheric conditions with slow stirring and a solution of ascorbic acid (0.037 M, Sigma-Aldrich, USA) was subsequently added as a reducing and capping agent under moderate stirring (generating a dark brown solution). Then, the reaction mixture was heated to 95°C in order to start a reflux, which was left for only 30 min under vigorous stirring, resulting in a red intensive color solution (which suggested a promoted reduction of Cu ions). The reaction solution was then slowly cooled to room temperature (RT) under moderate stirring for 1 h. Afterwards, the reacted solution was allowed to precipitate overnight. The supernatant was carefully removed, and the CuNPs precipitated were washed in absolute ethanol and dried overnight in a desiccator.

2.2. Physicochemical Characterization of CuNPs. In order to evaluate the structural morphology, homogeneity, size and degree of dispersion of the synthesized CuNPs, and 10 μL of CuNPs suspended in absolute ethanol were sampled on a double-sided adhesive carbon conductive tape, allowed to dry at RT, and characterized by means of field-emission scanning electron microscopy (FE-SEM; LYRA 3, Tescan, Brno, Czech Republic), at 10 kV accelerating voltage using a secondary electron detector. For the chemical composition analysis, energy dispersive X-ray spectroscopy (EDX, Tescan) measurements were carried out at 10 kV with a large spot size to adjust a suitable count rate per second for spectrum collection using an EDX coupled to the FE-SEM. The CuNPs were analyzed by Raman spectroscopy (Raman Station 400F Perkin-Elmer) at RT using a 785 nm diode laser beam at a power of 15 mW. The ultraviolet-visible (UV-Vis) spectra were acquired by suspending the CuNPs into deionized water (DI) and scanned in the wavelength region of 300 to 800 nm with a resolution of 1 nm at RT, using an UV/Vis spectrophotometer (UV-2600, Shimadzu, Japan). A dark-field illumination system (Cytoviva® 150 Resolution Imaging System, Auburn, AL, USA) equipped in a vertical microscope (Olympus BX-41, Japan) with a 100x oil immersion objective (Olympus, Japan) was used to observe the presence of CuNPs. 10 μL of CuNPs was then deposited on a slide with a coverslip, sealed with nail polish (to prevent drying), and mounted in the Cytoviva for imaging micrographs of the surface plasmon resonance (SPR) of CuNPs created by the integrated high signal-to--noise, dark field-based illumination. The size distribution (hydrodynamic diameter), zeta potential (ZP), and polydispersity index (PDI) of the CuNPs were analyzed by dynamic light scattering (DLS). For the DLS analysis, an aqueous suspension of 1.6 mg/L of CuNPs was sonicated in an ultrasonic bath (Branson, USA) at RT for 30 min. Next, the sonicated suspension was filtered (Whatman) and analyzed using a Nanotrac Wave II (Microtrac, North Wales, PA, USA) system with a zero time of 30 s and a run time of 30 s at RT.

2.3. C. albicans Culture. To carry out the antifungal analyses, we used a purified *C. albicans* strain isolated (before the antifungal treatment) from a 62 years old female patient that was clinically diagnosed with chronic atrophic oral denture candidiasis [21, 22]. For the preparation of the working inoculum, discrete colonies of freshly grown *C. albicans* were

inoculated into newly prepared Sabouraud dextrose broth (SDB; Becton Dickinson, USA) and were allowed to grow overnight under standard aerobic incubation conditions. Next, the *C. albicans* inoculum was diluted in SDB to approximately 1×10^7 colony-forming units (CFU)/mL, equivalent to an optical density (O.D.) of 1 at 590 nm, which was used for the antifungal evaluation tests.

2.4. Antifungal Evaluation. The microdilution method was selected and performed in a sterile 96-well flat bottom culture polystyrene plate (Corning, USA). Initially, 100 μL of fresh SDB was deposited into individual wells of the 96-well plate. Prior to the antifungal test, the CuNPs were suspended in sterile SDB to give a concentration of 2 mg/mL. The suspended CuNP solution was serially diluted (1000 μg/mL–7.81 μg/mL) into the 96-well plate containing the SDB. In order to test the antifungal capability of the CuNPs, 20 μL of the previously diluted *C. albicans* inoculum was deposited into each well (containing the CuNPs) of the 96-well and incubated under static conditions at 37°C in a humidified incubator for 24 h and 48 h, individually. After each incubation time, the experimental samples were placed in a microplate reader (Thermoskan, Thermo Fisher Scientific, USA) and the O.D. was measured at 590 nm. Separate cultures of medium free of CuNPs and SDB containing the same experimental concentrations of CuNPs without *C. albicans* were incubated under similar conditions and used as a control and baseline control, respectively. As an endeavor to evaluate the promoted antifungal capability of the CuNPs, a $CuCO_3$ precursor and the antifungal drug triclosan (selected as a positive control of antifungal activity) were compared under similar conditions of those of CuNPs.

2.5. In Situ Antifungal Behavior by Cytoviva®. For the characterization of the in situ cellular uptake and interaction of CuNPs, the Cytoviva® high-resolution system was used. After exposing *C. albicans* for 24 h and 48 h to 500 μg/mL of CuNPs, the cells were washed twice with warm PBS. The cellular suspension was then deposited (15 μL) onto a clean glass slide (VWR, USA), covered with a 0.145 mm thick glass cover slip (VWR, USA) and adhered using nail polish. The prepared slides were mounted and analyzed using the Cytoviva® system equipped with a high numerical 100x/1.30 oil Iris (Iris 1.3-0.6) immersion objective, for high-resolution imaging. The enhanced dark-field micrographs were analyzed using the ImageJ software (NIH, USA). Importantly, we did not apply any fixing technique in order to keep the intact cellular structure and accurately evaluate the NP uptake/interaction by the cells. Cellular suspensions treated by separate with $CuCO_3$ and triclosan (500 μg/mL) were evaluated using Cytoviva® for the characterization of structural *C. albicans* alterations, as described above. A culture of *C. albicans* prepared only in SDB was used as a positive control of cellular morphology.

2.6. Cytotoxicity (Viability) Assessment. In order to evaluate the cytotoxic (viability) profile of CuNPs, $CuCO_3$, and triclosan, we used primary human gingival fibroblasts (HGF) as a proper model of the cytotoxicity test [23–25]. The HGF were isolated from a clinically healthy young (15 years old) male patient as previously reported [26, 27]. Initially, 1×10^4 cells/-well were cultured in complete medium constituted of Dulbecco's modified Eagle's medium (DMEM, Thermo Fisher Scientific, USA) supplemented with 10% heat-inactivated fetal bovine serum (Thermo Fisher Scientific, USA) and 100 unit/mL of penicillin-streptomycin (Thermo Fisher Scientific, USA) in a 96-well culture flat bottom polystyrene plate (Corning, USA) at 37°C in a humidified 5% CO_2 incubator for 24 h, to form a monolayer. Next, the cells were washed twice for 5 min with warm PBS and incubated with serial dilutions (1000 μg/mL–7.81 μg/mL) of the testing compounds dissolved in complete a culture medium for 24 h. Afterwards, the cells were carefully washed twice with warm PBS, in order to eliminate the remaining substances. For the analytical cytotoxic test, 100 μL of MTT (3-(4,5-dimethylthiazol-2-yl)-2,5-diphenyl tetrazolium bromide, Sigma-Aldrich, USA) in complete medium (5 mg/mL) was added to each well of the cultured 96-well plate and incubated at 37°C for 4 h. For the dissolution of the produced formazan crystals (generated by mitochondrial activity), the remaining medium containing MTT was removed and the 96-well plate was transferred into an orbital incubator at 200 rpm and 37°C with 200 μL of dimethyl sulfoxide (Sigma-Aldrich, USA) into each well for 20 min. The O.D. of the dissolved crystals was then recorded at 590 nm using a microplate reader (Thermoskan, Thermo Fisher Scientific). For the determination of the baseline controls, a series of culture wells containing CuNPs, $CuCO_3$, and triclosan separately were carried out for MTT without fibroblasts as mentioned above, and cells without any testing compound were selected as a negative control of cytotoxicity. Moreover, the dose concentration-dependent data at which 50% of cell growth viability is inhibited (IC_{50}) was calculated by applying a nonlinear regression curve fit using GraphPad Prism 7.03.

2.7. Statistical Analysis. The experimental data were statistically analyzed by two-way analysis of variance (ANOVA) followed by Turkey's multiple comparison test. A $P < 0.05$ was considered statistically significant. GraphPad Prism 7 software (GraphPad Inc., USA) was used as the statistical package. Numerical data were expressed as the mean ± standard deviation (SD) of three independent experiments performed each in triplicate.

3. Results and Discussion

The SEM evaluation (Figure 1) illustrated that our synthesis route resulted in the formation of homogenous and well-dispersed CuNPs. The spherical morphology of CuNPs was approximately 250 nm in size due to the ascorbic acid cap wrapping the metallic copper nanoparticles. Moreover, we observed few remaining nucleation zones among the CuNPs. Information suggested an appropriate distribution of the CuNPs and that the thermodynamic conditions of our synthesis method were favorable for the proper growth of the NPs, as advised by others [28, 29]. The EDX analysis (see inserted table in Figure 1) showed that the main elements remaining after the synthesis of the CuNPs were

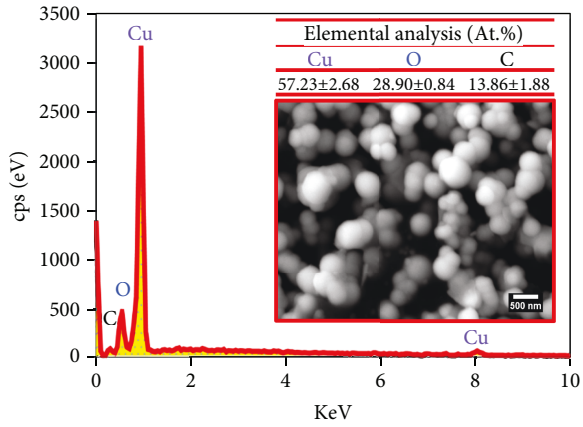

Figure 1: Physicochemical characterization of the synthesized CuNPs. The inserted table shows the elemental composition of the CuNPs.

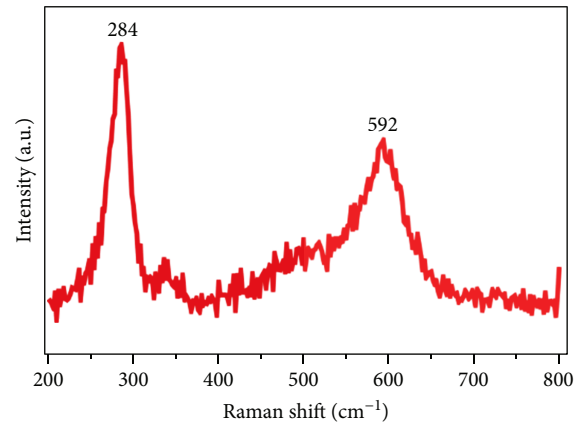

Figure 2: Raman spectrum of the synthesized CuNPs.

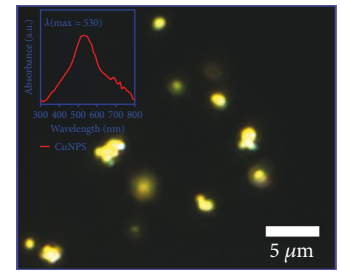

Figure 3: Enhanced dark-field micrograph generated from the CuNPs. The inserted graph represents the UV-Vis analysis of the CuNPs.

Cu (57.23 ± 2.68%), O (28.90 ± 0.84%), and C (13.86 ± 1.88%). It is important to take into consideration that our synthesis process used ascorbic acid as the reducer and stabilizer agent, which allowed the formation of stable CuNPs with a consistent spherical shape [28, 30]. Furthermore, the natural antioxidant ability of ascorbic acid is an important advantage for the protection against the oxidation of CuNPs. The antioxidant property allows scavenging of free radicals and acts as an intermediate during donation of electrons in a redox reaction [13]. The scavenger capability of the ascorbic acid also facilitates the protection to the oxidation of a wide number of different organic and/or inorganic molecules [31]. Therefore, to avoid the oxidation of the CuNPs, an excess of ascorbic acid during the reaction was added. Thus, this information may explain in part the presence of oxygen and carbon (which could be attributed to organic elements from a cover film capping the copper nanoparticle) after the EDX analysis. On the other hand, the elevated concentration of Cu could be depicted to the formation of basically pure Cu^0-based NPs [13].

During the synthesis of the CuNPs, a color change from a dark-brown solution (formed after the immediate contact with ascorbic acid) to a reddish-brown after the reflux was visualized, indicating the formation of stable CuNPs [12, 32]. Thus, we applied UV-Vis analysis and detected that the SPR band of our NPs was at 530 nm (Figure 2, see inset), due to a possible transition movement of the valence electron of Cu. Interestingly, our spectrum showed only one high and intense peak (at 530 nm), without any superimposition at any close wavelength. This data may support that mostly all CuNPs were dispersed (as supported by SEM) with a low molecular fragmentation, which in turn indicates a greater capping of the nanoparticles (outcomes of NP stability) [28, 33]. Moreover, the slight shifted wavelength (≈50 nm) observed for our CuNPs may be attributed to the free π electrons provided by the ascorbic capper that collectively reacts with the SPR of the CuNPs. The modest shift detected for our CuNPs is in concordance to a previous study of CuNPs synthesized using glucosamine as an organic capper [34]. The authors reported a shifted SPR of 577 nm (from CuNPs without glucosamine) to 525 nm after the capping with glucosamine. Furthermore, a Raman analysis over our CuNPs (Figure 3) suggested the presence of minor levels of CuO. This data may also propose that the moderate wavelength shifted could be associated together with negligible levels of oxidized CuNPs. However, more analytical studies are recommended in order to explain this interesting behavior. In addition to the UV-Vis and SEM measurements, the dark-field micrographs reinforced the above-mentioned results. The CuNPs also continued showing a dispersed distribution with a homogenous spherical shape, as presented by the SPR detected and captured with the Cytoviva® system (Figure 2). To confirm the stability and distribution homogeneity of the CuNPs, the DLS scanning with Z potential analysis was carried out (Figure 4). The ZP obtained for the CuNPs was -24.7 mV. This ZP may suggest a great number of electrostatic repulsive forces between the colloidal suspension that could result in impaired absorption of negative ions and complex ligand interactions between the Cu^{+2} ions (reduced aggregation of the CuNPs) [11, 35]. Moreover, the presence of C and O from the ascorbic acid could also be contributed in the reduction of repulsive forces, showing a better stability with reduced agglomeration of the CuNPs, as evidenced from the ZP and DLS results. Following this proposed stability mechanism, we can postulate that our synthesized CuNPs are stable in nature [13]. However, more analytical studies are recommended in order to evaluate the

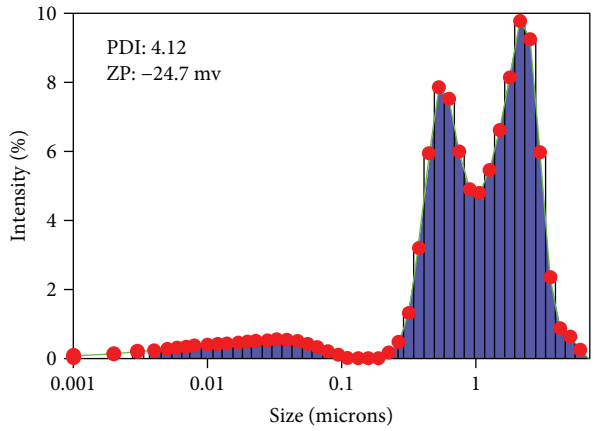

Figure 4: DLS evaluation with Z potential and polydispersity index of the CuNPs.

long-term stability of the CuNPs. The size distribution also indicated that the higher proportion of the CuNPs is among 250 nm (supporting SEM, see Figure 1) and the PDI suggested an acceptable dispersion.

According to the information from SEM, UV-Vis, EDX, Cytoviva®, DLS, and the suggested synthetic pathway proposed in Figure 5, we can postulate that the formation of spherical-shaped CuNPs is related to an initial fast reduction between the Cu^{+2} ions and the ascorbic acid. Also, the application of a constant reflux controlled the chemical reduction for the formation of well-distributed CuNPs. Additionally, the excess of ascorbic acid during the reflux reaction may help to modulate the nucleation and growth of the CuNPs during the process of the reduction (which could explain the color changes). In this synthesis, the nucleation and stabilization of the CuNPs take place simultaneously due to the capping process promoted by ascorbic acid. The aqueous dissolution of $CuCO_3$ dissociates to Cu^{+2} and CO_3^{-2}, while the mixture with ascorbic acid could take the free Cu^{+2} ions and easily start the reduction. As the reduction took place under reflux conditions, the elimination of CO_3^{-2} in the form of CO_2 (observed by the formation of bubbles during the reaction) and H_2O may be promoted, which leaves in the reaction mixture the presence of mainly pure CuNPs and H_2O.

As stated before, *C. albicans* is the most important and dangerous opportunistic fungal cell, responsible for a wide number of fungus-associated diseases [6]. When *C. albicans* colonized a biofilm, it presents a higher resistance against the most common pharmacotherapies. Hence, there is an important requirement of novel strategies for the development of antifungals aimed for the treatment of associated fungal infections (as those of *C. albicans*). Thus, in this study, we used as a model of fungal cells a wild pathogenic *C. albicans* strain isolated from an oral denture candidiasis. The results showed a dose-dependent response for the treatment with CuNPs after 24 h (Figure 6). It must be remarked that the CuNP treatment showed an initial significant reduction of the fungal viability when compared to the precursor, mainly appreciated at 250 μg/mL (see inset, Figure 6). Moreover, after 48 h of culture, we detected a sustained antifungal damage for the CuNPs (at all concentrations) when compared to the $CuCO_3$ precursor (Figure 7). It can be highlighted that the minimal inhibitory concentration (MIC) continued working at 500 μg/mL for CuNPs (as observed at 24 h). Also, we can hypothesize that the CuNPs require prolonged incubations in order to induce and keep a remarkable fungal impairment; information suggested that the CuNPs presented a similar initial antifungal behavior to that of $CuCO_3$, but an important antifungal activity after an extended treatment. On the other hand, triclosan (selected as a positive control of antifungal activity) is showed to absolutely inhibit *C. albicans* growth, as expected. Meanwhile, our CuNPs were capable to mimic this anticandida activity (after 500 μg/mL).

In order to approach part of the antifungal mechanism involved by the tested materials (mainly CuNPs), we applied enhanced dark-field microscopy (Figure 8), as a novel tool that offers the advantage to be used without any fixing (chemical or physical) or aggressive washing techniques [36]. At 24 h of incubation in the control well, we detected a well-established *C. albicans* growth showing the formation of pseudohifas and the presence of multinucleated cells (suggesting important viability and correct cellular grow). Moreover, after 48 h of incubation, the control showed a mature morphology (see the interconnection of the multinucleated hyphae and the giant yeast cells). Those results indicated that the incubation conditions used in this study were optimal for the fungal tests. On the other hand, at 24 and 48 h of evolution, the cellular morphology witnessed for the triclosan and $CuCO_3$ showed similar properties of a cellular shape to those of the control test. Most importantly, the CuNPs are indicated to bind to the cell wall (yellow arrows) in order to be capable to penetrate inside the fungal cells (Figure 8). As observed at 24 h, *C. albicans* illustrated the shape of mononucleated cells without the formation of pseudohifas (which could suggested genomic alterations by the nanomaterial treatment), and CuNPs also adhered to the nuclear membrane (as illustrated by the green arrows). Although the cells still conserved their yeast morphology, it is clearly observed that cellular leakage takes place due to the dispersed fragments and the formation of fibrils that were detected by the dark-field enhanced capacity. Thus, we can stipulate that the CuNPs originate slightly electrostatic bonds (as suggested by the ZP results) to the cellular wall that promotes the penetration (probably by permeabilization) of the CuNPs to the cytoplasm space, generating NP accumulation. The accumulation process will be maintained before the cell gets lysed (as observed after 48 h in the CuNPs treatment), promoting by this pathway a toxic accumulation of CuNPs in all the cellular compartments. Several studies have suggested that one of the most remarkable antimicrobial mechanisms that explain the action of metallic NPs (e.g., Ag, Au, or Cu) involves the formation of ROS (due to elevated concentration of OH radicals) by the contact of the NPs to the internal and membrane proteins [19, 20, 37]. Moreover, two interesting ultrastructural characterization reports (by TEM) using AgNPs and *C. albicans* proposed that AgNPs have to extensively accumulate at the cell membrane in order to penetrate it and by this way alter the cellular

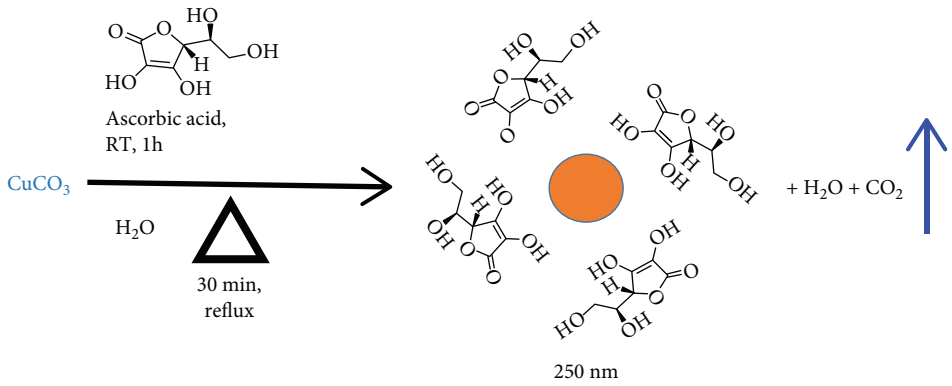

Figure 5: Schematic representation of the synthetic route designed for the synthesis of CuNPs.

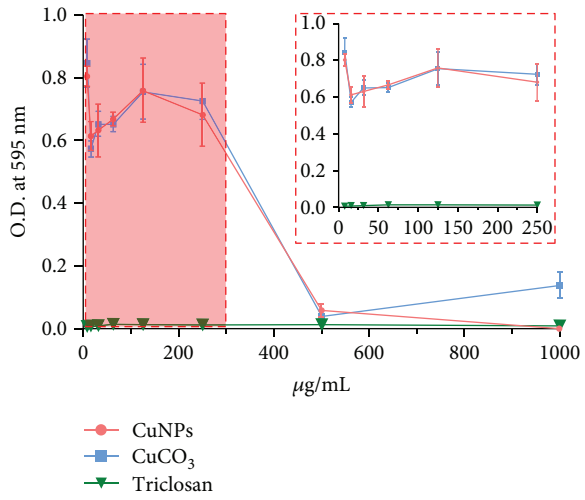

Figure 6: Dose-response analysis of the CuNPs and the positive and negative control versus *C. albicans* after 24 h of incubation. The inserted graph represents in detail the antifungal behavior from 7.8125 to 250 μg/mL.

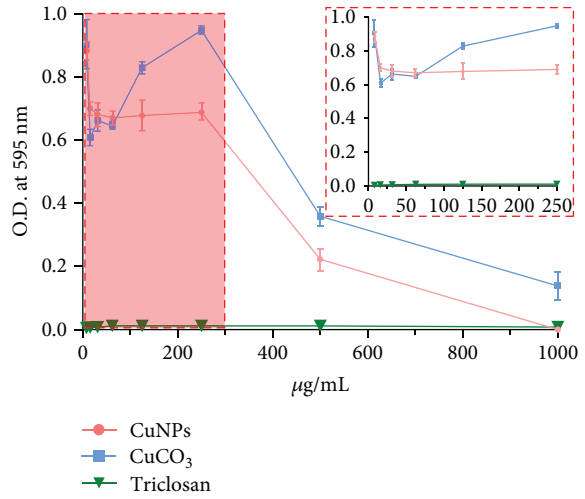

Figure 7: Graphical dose-response evaluation of the CuNPs and the positive and negative control against *C. albicans* after 48 h of growth. The included graph shows a detailed performance of the studied substances from 7.8125 to 250 μg/mL.

structure [38, 39]. However, those studies required the use of cross-linking fixatives and extensive washing techniques that may alter the original cellular morphology. Therefore, assuming the need of NP binding to the fungal surface, our results proposed that CuNP attachment and the *C. albicans* efflux can be more accurately evaluated by the application of the Cytoviva® system. Accordingly, taking together our results and the discussed ultrastructural and molecular analysis, we can hypothesize that contact between the CuNPs and *C. albicans* will mediate the NPs binding to the cell surface (especially the cell wall). The bound CuNPs will diffuse to the internal compartments, occasioning by this way an elevation of cellular stress by dynamic changes (due to the NPs accumulation) and enlarged production of ROS. Those important mechanisms will conclude cellular lysis by stress oxidation and cell membrane dissociation. On the other hand, it is important to discuss the role of the surface chemistry in the antifungal activity of our CuNPs. Our results showed the presence of C and O (mainly from the capping with ascorbic acid, see Figure 1), which in part contributed to a better stability of the CuNPs (as previously discussed) and improved antifungal activity. In a previous study, Veerapandian et al. synthesized antimicrobial CuNPs stabilized by glucosamine [34]. Their CuNPs showed elevated presence of C and O with similar SPR to those of our CuNPs. This information suggested the use of organic cappers as stabilizers of CuNPs with promoted antimicrobial activity. However, more studies are recommended in order to evaluate the main effect of the surface chemistry of CuNPs.

An important issue that must be seriously considered for the effective function of antimicrobial substances is the potent cytotoxic effects in mammalian cells. The results of the cytotoxicity tests (MTT) in the HGF (a primary cellular culture) showed that the IC_{50} values of the testing compounds (Figure 9) were as follows: CuNPs (137.4 μg/mL) < triclosan (77.25 μg/mL) < $CuCO_3$ (48.4 μg/mL). The IC_{50} observed for the CuNPs indicated that our reduction protocol decreased more than 2.8 folds the toxicity of the Cu precursor. This data suggests that the use of ascorbic acid as a stabilizer, reducer, and capping agent could improve the tolerance of Cu in human tissue cultures. Moreover, the IC_{50} presented for the triclosan (used as a positive control of antifungal activity) was almost 1.78 folds inferior to that of the CuNPs, which

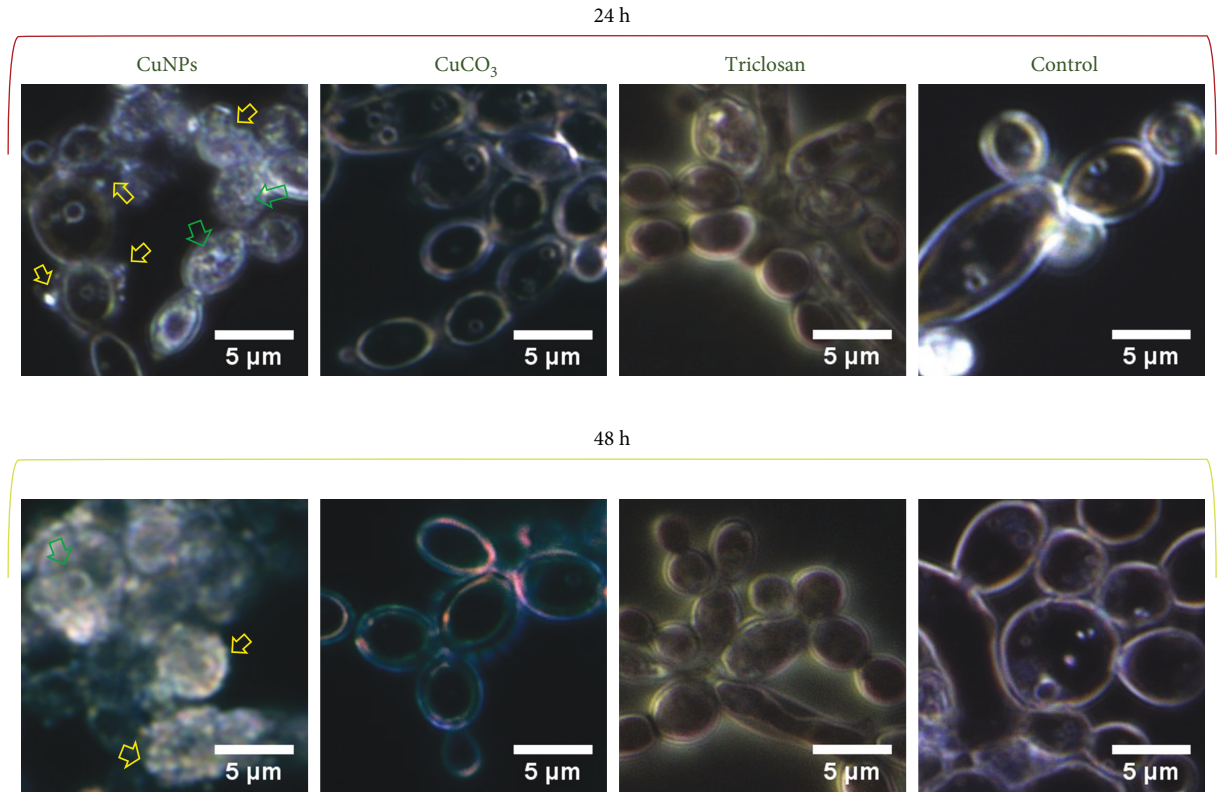

Figure 8: Enhanced dark-field micrographs showing the cellular morphology of the experimental treatments at 24 and 48 h of incubation. The yellow arrows highlight the presence of adhered CuNPs to the cell wall. The green arrows remark the localization and accumulation of CuNPs at the periphery of the nuclear membrane.

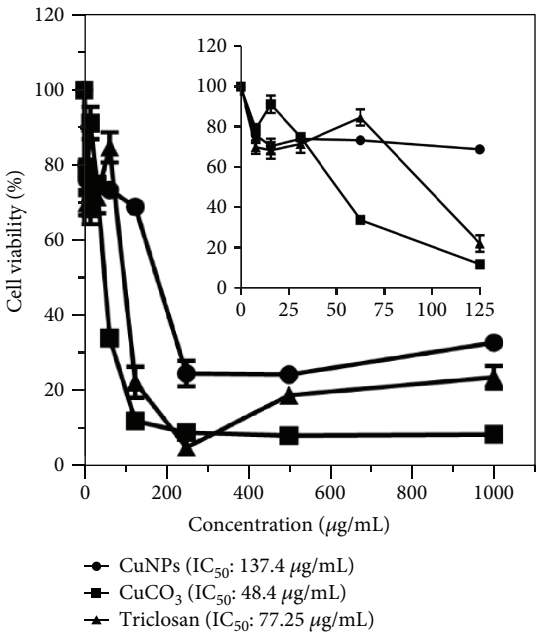

Figure 9: Dose-response curve for the IC_{50} values after 24 h of culture with the experimental solutions.

suggests that our CuNPs could be used at higher concentrations compared to the antifungal drug. To the best of our knowledge, this is the first study presenting a promoted biocompatibility obtained for Cu nanoparticles, after a chemical reduction using a Cu precursor. Also, our cytotoxic test illustrated a dose-dependent behavior for all the substances (Figures 9 and 10). Surprisingly, the $CuCO_3$ precursor was the most cytotoxic substance, presenting a predominantly reduced viability at concentrations lower than 62.5 μg/mL (see Figure 10). The superior cytotoxicity witnessed for the Cu precursor could be related to a bulk delivery of Cu^{+2} ions directly into the cultured cells [40]. A previous study suggested elevated cytotoxicity of human epithelial cells (HEp-2) at concentrations of 80 μg/mL for CuNPs, in part by the higher accumulation of Cu ions into the HEp-2 cells [40, 41]. Moreover, a genotoxic study in epithelial cells suggested superior outcomes of cellular stress due to the presence of low concentrations of CuNPs (50 μg/mL). The genotoxic effect was in part associated to the increased levels of Cu ions (from CuNPs) inside the cells, which may elevate oxidative stress via lipid peroxidation and DNA damage [41]. On the other hand, triclosan presented a higher cellular acceptability compared to the $CuCO_3$, as it showed a significantly prominent viability (up to 80% for 62.5 μg/mL). In Figure 9, an enhanced cellular viability for almost all the experimental concentrations tested for the CuNPs can be analyzed. This interesting trend is followed by the triclosan and finally by the Cu precursor. Furthermore, we appreciated a promoted cellular viability (70%) beginning at the elevated concentration of 125 μg/mL for the CuNPs (Figure 10). However, the triclosan and the $CuCO_3$ were able to reach this cell viability

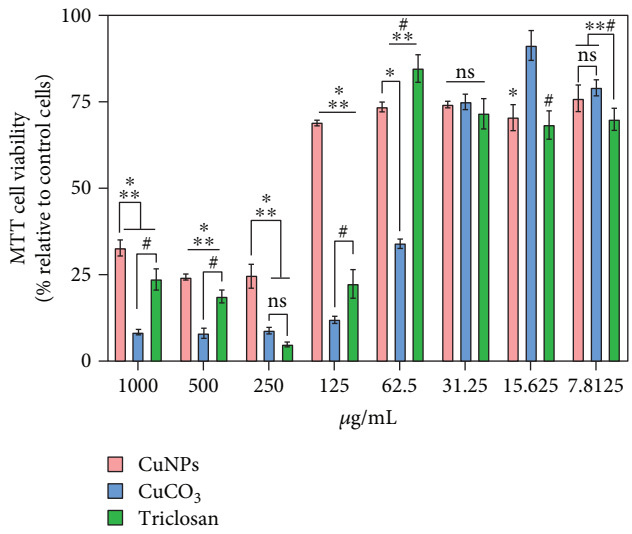

Figure 10: Cellular viability after 24 h of exposure with CuNPs, $CuCO_3$, and triclosan. Results represent the means ± standard deviations. * illustrates significant differences between CuNPs and $CuCO_3$. ** shows significant changes among the CuNPs and Triclosan. # points out differences between $CuCO_3$ and triclosan.

at concentrations of 62. 5 μg/mL and 31.25 μg/mL, respectively. Although the CuNP results showed interesting outcomes of promoted and sustained antifungal activity and reduced cellular toxicity, more molecular studies are recommended in order to fully elucidate the mechanism postulated here.

4. Conclusions

The present study showed a new synthetic route for the synthesis of uniform and dispersed antifungal CuNPs using a facile, cost-effective, and eco-friendly chemical reduction approach. Moreover, our results brings new evidence of the antifungal mechanism of CuNPs against an important fungal model. The synthesized CuNPs showed a homogenous spherical morphology with a prominent level of Cu associated to Cu^0 generated by the reduction protocol. Also, slight concentrations of C and O were detected, which could be associated to the ascorbate capping. Our CuNPs were capable to reduce the colonization of *C. albicans* after 24 h and even 48 h of culture. The application of enhanced dark-field microscopy allowed to hypothesize part of the antifungal mechanism. It is proposed that CuNPs are capable to adhere to the surface of the cell wall and by this way promote a permeabilization that allows the internment of CuNPs into the cytoplasm. The CuNPs accumulate among the intercellular space (48 h) and the surface of the nuclear membrane, probably inducing that *C. albicans* maintain the yeast morphology (which reduce the survival rate). Moreover, the CuNPs may encourage the dysfunction of internal proteins followed by elevated production of ROS. Although our CuNPs were highly antifungal, the cytotoxicity profile showed the most reduced outcomes of metabolic cell dysfunction for the CuNPs, followed by the triclosan and the $CuCO_3$ suggesting that the reduction protocol may protect the cellular integrity against Cu^{+2} ions. Our results provide significant evidence that open up a new road for the use of CuNPs as a potent tool for clinical, antimicrobial, and industrial applications. Moreover, the results propose the use of enhanced dark-field microscopy as a potent and valuable tool for the characterization of the antifungal mechanism of different NPs.

Data Availability

The data used to support the findings of this study are included within the article.

Disclosure

The founding sponsors had no role in the design of the study; in the collection, analyses, or interpretation of data; in the writing of the manuscript; or in the decision to publish the results.

Conflicts of Interest

The authors declare no conflict of interest.

Acknowledgments

The authors thank the Autonomous University of Baja California for grant 2060 provided by 19va Convocatoria Interna de Apoyos a Proyectos de Investigación, funding 25770 to UABC CA-276 afforded by Apoyo al Fortalecimiento de Cuerpos Académicos 2017 SEP-PRODEP.

References

[1] N. Høiby, T. Bjarnsholt, M. Givskov, S. Molin, and O. Ciofu, "Antibiotic resistance of bacterial biofilms," *International Journal of Antimicrobial Agents*, vol. 35, no. 4, pp. 322–332, 2010.

[2] H. Koo, R. N. Allan, R. P. Howlin, P. Stoodley, and L. Hall-Stoodley, "Targeting microbial biofilms: current and prospective therapeutic strategies," *Nature Reviews Microbiology*, vol. 15, no. 12, pp. 740–755, 2017.

[3] A. K. Thabit, J. L. Crandon, and D. P. Nicolau, "Antimicrobial resistance: impact on clinical and economic outcomes and the need for new antimicrobials," *Expert Opinion on Pharmacotherapy*, vol. 16, no. 2, pp. 159–177, 2015.

[4] A. K. Guitor and G. D. Wright, "Antimicrobial resistance and respiratory infections," *Chest*, vol. 154, no. 5, pp. 1202–1212, 2018.

[5] M. Selvaraj, P. Pandurangan, N. Ramasami, S. B. Rajendran, S. N. Sangilimuthu, and P. Perumal, "Highly potential antifungal activity of quantum-sized silver nanoparticles against Candida albicans," *Applied Biochemistry and Biotechnology*, vol. 173, no. 1, pp. 55–66, 2014.

[6] M. B. Lohse, M. Gulati, A. D. Johnson, and C. J. Nobile, "Development and regulation of single- and multi-species Candida albicans biofilms," *Nature Reviews Microbiology*, vol. 16, no. 1, pp. 19–31, 2017.

[7] S. Rasch, U. Mayr, V. Phillip et al., "Increased risk of candidemia in patients with necrotising pancreatitis infected with candida species," *Pancreatology*, vol. 18, no. 6, pp. 630–634, 2018.

[8] M. Kollef, S. Micek, N. Hampton, J. A. Doherty, and A. Kumar, "Septic shock attributed to Candida infection: importance of empiric therapy and source control," *Clinical Infectious Diseases*, vol. 54, no. 12, pp. 1739–1746, 2012.

[9] J. Ramyadevi, K. Jeyasubramanian, A. Marikani, G. Rajakumar, and A. A. Rahuman, "Synthesis and antimicrobial activity of copper nanoparticles," *Materials Letters*, vol. 71, pp. 114–116, 2012.

[10] A. Khan, A. Rashid, R. Younas, and R. Chong, "A chemical reduction approach to the synthesis of copper nanoparticles," *International Nano Letters*, vol. 6, no. 1, pp. 21–26, 2016.

[11] J. Yu, J. Nan, and H. Zeng, "Size control of nanoparticles by multiple-pulse laser ablation," *Applied Surface Science*, vol. 402, pp. 330–335, 2017.

[12] T.-Y. Lin, Y. L. Chen, C. F. Chang et al., "*In situ* investigation of defect-free copper nanowire growth," *Nano Letters*, vol. 18, no. 2, pp. 778–784, 2018.

[13] P. Gurav, S. S. Naik, K. Ansari et al., "Stable colloidal copper nanoparticles for a nanofluid: production and application," *Colloids and Surfaces A: Physicochemical and Engineering Aspects*, vol. 441, pp. 589–597, 2014.

[14] N. A. Dhas, C. P. Raj, and A. Gedanken, "Synthesis, characterization, and properties of metallic copper nanoparticles," *Chemistry of Materials*, vol. 10, no. 5, pp. 1446–1452, 1998.

[15] M. Ben-Sasson, K. R. Zodrow, Q. Genggeng, Y. Kang, E. P. Giannelis, and M. Elimelech, "Surface functionalization of thin-film composite membranes with copper nanoparticles for antimicrobial surface properties," *Environmental Science & Technology*, vol. 48, no. 1, pp. 384–393, 2014.

[16] M. Raffi, S. Mehrwan, T. M. Bhatti et al., "Investigations into the antibacterial behavior of copper nanoparticles against Escherichia coli," *Annals of Microbiology*, vol. 60, no. 1, pp. 75–80, 2010.

[17] M. Goswami and A. M. Das, "Synthesis of cellulose impregnated copper nanoparticles as an efficient heterogeneous catalyst for CN coupling reactions under mild conditions," *Carbohydrate Polymers*, vol. 195, pp. 189–198, 2018.

[18] X. Yan, B. He, L. Liu et al., "Antibacterial mechanism of silver nanoparticles in Pseudomonas aeruginosa: proteomics approach," *Metallomics*, vol. 10, no. 4, pp. 557–564, 2018.

[19] S. Agnihotri, S. Mukherji, and S. Mukherji, "Size-controlled silver nanoparticles synthesized over the range 5–100 nm using the same protocol and their antibacterial efficacy," *RSC Advances*, vol. 4, no. 8, pp. 3974–3983, 2014.

[20] C. Arijit Kumar, C. Ruchira, and B. Tarakdas, "Mechanism of antibacterial activity of copper nanoparticles," *Nanotechnology*, vol. 25, no. 13, article 135101, 2014.

[21] M. A. Pfaller, A. Houston, and S. Coffmann, "Application of CHROMagar Candida for rapid screening of clinical specimens for Candida albicans, Candida tropicalis, Candida krusei, and Candida (Torulopsis) glabrata," *Journal of Clinical Microbiology*, vol. 34, no. 1, pp. 58–61, 1996.

[22] E. Beltrán-Partida, B. Valdez-Salas, M. Curiel-Álvarez, S. Castillo-Uribe, A. Escamilla, and N. Nedev, "Enhanced antifungal activity by disinfected titanium dioxide nanotubes via reduced nano-adhesion bonds," *Materials Science and Engineering: C*, vol. 76, pp. 59–65, 2017.

[23] R. P. Illeperuma, Y. J. Park, J. M. Kim et al., "Immortalized gingival fibroblasts as a cytotoxicity test model for dental materials," *Journal of Materials Science: Materials in Medicine*, vol. 23, no. 3, pp. 753–762, 2012.

[24] W. Geurtsen, F. Lehmann, W. Spahl, and G. Leyhausen, "Cytotoxicity of 35 dental resin composite monomers/additives in permanent 3T3 and three human primary fibroblast cultures," *Journal of Biomedical Materials Research*, vol. 41, no. 3, pp. 474–480, 1998.

[25] Y. Yang, F.-X. Reichl, J. Shi, X. He, R. Hickel, and C. Högg, "Cytotoxicity and DNA double-strand breaks in human gingival fibroblasts exposed to eluates of dental composites," *Dental Materials*, vol. 34, no. 2, pp. 201–208, 2018.

[26] J. J. Aleo, F. A. de Renzis, and P. A. Farber, "In vitro attachment of human gingival fibroblasts to root surfaces," *Journal of Periodontology*, vol. 46, no. 11, pp. 639–645, 1975.

[27] K. J. Baek, Y. Choi, and S. Ji, "Gingival fibroblasts from periodontitis patients exhibit inflammatory characteristics in vitro," *Archives of Oral Biology*, vol. 58, no. 10, pp. 1282–1292, 2013.

[28] D. Mott, J. Galkowski, L. Wang, J. Luo, and C.-J. Zhong, "Synthesis of size-controlled and shaped copper nanoparticles," *Langmuir*, vol. 23, no. 10, pp. 5740–5745, 2007.

[29] W. Luo, W. Hu, and S. Xiao, "Size effect on the thermodynamic properties of silver nanoparticles," *The Journal of Physical Chemistry C*, vol. 112, no. 7, pp. 2359–2369, 2008.

[30] C. Salzemann, I. Lisiecki, J. Urban, and M. P. Pileni, "Anisotropic copper nanocrystals synthesized in a supersaturated medium: nanocrystal growth," *Langmuir*, vol. 20, no. 26, pp. 11772–11777, 2004.

[31] S.-Y. Xie, Z.-J. Ma, C.-F. Wang et al., "Preparation and self-assembly of copper nanoparticles via discharge of copper rod electrodes in a surfactant solution: a combination of physical and chemical processes," *Journal of Solid State Chemistry*, vol. 177, no. 10, pp. 3743–3747, 2004.

[32] U. Bogdanović, V. Vodnik, M. Mitrić et al., "Nanomaterial with high antimicrobial efficacy—copper/polyaniline nanocomposite," *ACS Applied Materials & Interfaces*, vol. 7, no. 3, pp. 1955–1966, 2015.

[33] D. Gozzi, M. Tomellini, L. Lazzarini, and A. Latini, "High--temperature determination of surface free energy of copper nanoparticles," *The Journal of Physical Chemistry C*, vol. 114, no. 28, pp. 12117–12124, 2010.

[34] M. Veerapandian, S. Sadhasivam, J. Choi, and K. Yun, "Glucosamine functionalized copper nanoparticles: preparation, characterization and enhancement of anti-bacterial activity by ultraviolet irradiation," *Chemical Engineering Journal*, vol. 209, pp. 558–567, 2012.

[35] M. Muniz-Miranda, C. Gellini, and E. Giorgetti, "Surface-enhanced Raman scattering from copper nanoparticles obtained by laser ablation," *The Journal of Physical Chemistry C*, vol. 115, no. 12, pp. 5021–5027, 2011.

[36] H. Weinkauf and B. F. Brehm-Stecher, "Enhanced dark field microscopy for rapid artifact-free detection of nanoparticle binding to Candida albicans cells and hyphae," *Biotechnology Journal*, vol. 4, no. 6, pp. 871–879, 2009.

[37] I.-s. Hwang, J. Lee, J. H. Hwang, K.-J. Kim, and D. G. Lee, "Silver nanoparticles induce apoptotic cell death in Candida albicans through the increase of hydroxyl radicals," *The FEBS Journal*, vol. 279, no. 7, pp. 1327–1338, 2012.

[38] R. Vazquez-Muñoz, M. Avalos-Borja, and E. Castro-Longoria, "Ultrastructural analysis of Candida albicans when exposed to silver nanoparticles," *PLoS One*, vol. 9, no. 10, article e108876, 2014.

[39] H. H. Lara, D. G. Romero-Urbina, C. Pierce, J. L. Lopez-Ribot, M. J. Arellano-Jiménez, and M. Jose-Yacaman, "Effect of silver nanoparticles on Candida albicans biofilms: an ultrastructural study," *Journal of Nanobiotechnology*, vol. 13, no. 1, p. 91, 2015.

[40] B. Fahmy and S. A. Cormier, "Copper oxide nanoparticles induce oxidative stress and cytotoxicity in airway epithelial cells," *Toxicology In Vitro*, vol. 23, no. 7, pp. 1365–1371, 2009.

[41] M. Ahamed, M. A. Siddiqui, M. J. Akhtar, I. Ahmad, A. B. Pant, and H. A. Alhadlaq, "Genotoxic potential of copper oxide nanoparticles in human lung epithelial cells," *Biochemical and Biophysical Research Communications*, vol. 396, no. 2, pp. 578–583, 2010.